

Structure-function relation in the coronary artery tree: from fluid dynamics to arterial bifurcations

G rard Finet^{1*}, MD, PhD; Yunlong Huo², PhD; Gilles Rioufol¹, MD, PhD; Jacques Ohayon³, PhD; Patrice Guerin⁴, MD, PhD; Ghassan S. Kassab², PhD

1. *D partement of Interventional Cardiology, Cardiovascular Hospital and Claude Bernard University, and INSERM 886, Lyon, France;* 2. *Department of Biomedical Engineering, Indiana-Purdue University, Indianapolis, IN, USA;* 3. *Laboratory TIMC-IMAG, DynaCell, CNRS UMR 5525, Institut de l'Ing nierie et de l'Information de Sant  (In3S), Grenoble, France;* 4. *INSERM UMR915, Institut du Thorax, Service d'H modynamique, and Centre Commun de Microscopie Electronique, Nantes, France*

The authors have no conflict of interest to declare.

"With a fractal, you look in and in and in and it always goes on being fractal. It's a way towards a greater awareness of unity."

David Hockney

Introduction

Coronary artery bifurcations have a predilection for atherosclerosis for which the percutaneous treatment is complex. Bifurcations are anatomic-functional transitions within the coronary artery tree structure which fulfill a distributive function. The objective of this review is to outline the structure-function relations of coronary bifurcations as a rationale for percutaneous treatment of these complex lesions.

The fractal nature of vascular trees

Coronary artery bifurcations are an elegant solution to the question of 3-dimensional (3-D) spatial distribution of blood-flow throughout the myocardium¹. An optimal physiological arrangement involves a finite (and, ideally, small) volume of blood that must be metabolically exchanged over a very large surface area (level of cells). Although Euclidean geometry fails to meet this objective, such an arrangement is well within the realm of fractal geometry; i.e., scale-independent, self-similarity of bifurcation pattern in the 3-D vascular architecture².

Fractal structures are composed by a recursive pattern reproduced to generate invariable self-similarity regardless of the scale of observation. Such structure tends to maximise the occupation of a finite volume, without interference between the elements of the fractal pattern. For example, the further you go in a fractal, the longer it gets, whereas the further you go in a circle the more quickly the limit is reached. The underlying concepts in a fractal geometry are "form", "chance" and "dimension". "Form" is what can be seen as a whole; i.e., an object of immediate perception. "Chance" comes to play in the simulation and synthesis of such a form. Finally, "dimension" characterises fractal objects. Mandelbrot developed this new geometry to describe natural phenomena called fractal geometry. It was in 1975 that he coined the term fractal, from the Latin *frangere* (to break). Nature has indeed created "objects" of seemingly remarkable complexity in their expression or analytic description. Seen as fractal objects, on the other hand, these natural objects can be described with remarkable simplicity, requiring a recurrent ratios or exponents.

The fractal nature of coronary tree geometry has long been recognised³⁻⁵ as illustrated for epicardial arteries in Figure 1. Tanaka et al⁶, using micro-angiography by synchrotron radiation, demonstrated the self-similarity of the intra-myocardial branching pattern for diameters between 50 and 500 μm .

* Corresponding author: Department of Interventional Cardiology, Cardiovascular Hospital, B.P Lyon-Monchat, 69394 Lyon Cedex 03, France
E-mail: gerard.finet@univ-lyon1.fr

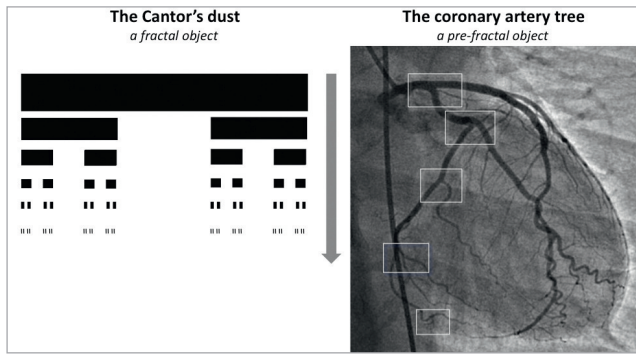


Figure 1. Fractal and prefractal objects. A) The theoretical fractal object known as Cantor dust is a good illustration of fractal geometry. Consider an initial segment, remove the mid-third and then the mid-thirds of the remaining segments, and so on, iteratively. The Cantor set is the dust of the resulting points. Their number is infinite, but their total length zero. Such Cantor dusts cannot be described in Euclidean geometry. They are lacunate, complex, riddled structures. B) The coronary artery tree. Arterial arborescence creates an apparently complex lacunate structure providing a very large area of content (blood) exchange and diffusion within a finite volume (coronary artery).

Arterial bifurcations have a 3D blood-distribution function

If the function dictates the organ, blood-flow distribution dictates vascular geometry. According to the law of conservation of mass, the sum of the outflows from a bifurcation equals the inflow. Flow (Q) is related to lumen cross-sectional area (A) by flow velocity (V) such that $Q=A \cdot V$. This clearly points to a relation between function (blood flow) and geometry (cross-sectional diameter and area).

There are many theories of vascular tree design based on the concept of minimum work^{7,8}. The preoccupation is to understand what dictates the lumen dimension of a vessel based on the principle of efficiency (i.e., energy required to circulate the blood is minimised). In this regard, Murray proposed a cost function that is the sum of friction power loss and metabolic power dissipation proportional to blood volume⁷. The consequence of this minimum energy hypothesis is Murray's law⁷, also known as the cube law, which states that the sum of the cubes of the daughter-vessel diameters (D_{d1} and D_{d2}) is equal to the cube of the mother-vessel diameter (D_m) as: $D_m^3 = D_{d1}^3 + D_{d2}^3$. Kassab and colleagues⁸⁻¹⁰ showed that Murray's law does not hold in the entire tree as Murray's analysis considered each bifurcation in isolation rather than as an integrated whole. The latter treatment results in a 7/3 exponent referred to as HK model¹¹: i.e., $D_m^{7/3} = D_{d1}^{7/3} + D_{d2}^{7/3}$ which has been rigorously validated⁸⁻¹¹. Finally, Finet et al¹² (Figure 2) observed a linear relation ($D_m = 0.678 * [D_{d1} + D_{d2}]$) based on regression analysis of Y-type bifurcation which has elegance of simplicity (i.e., 0.678 expresses the ratio of mother diameter to the sum of daughter diameters). Interestingly, the HK model gives rise to a ratio of 0.673 for the case of equal diameter of daughter vessels (Y-bifurcation). Hence, the HK model is not only consistent with the Finet rule for Y-bifurcations but also hold for T-bifurcations which were not considered in Finet et al¹².

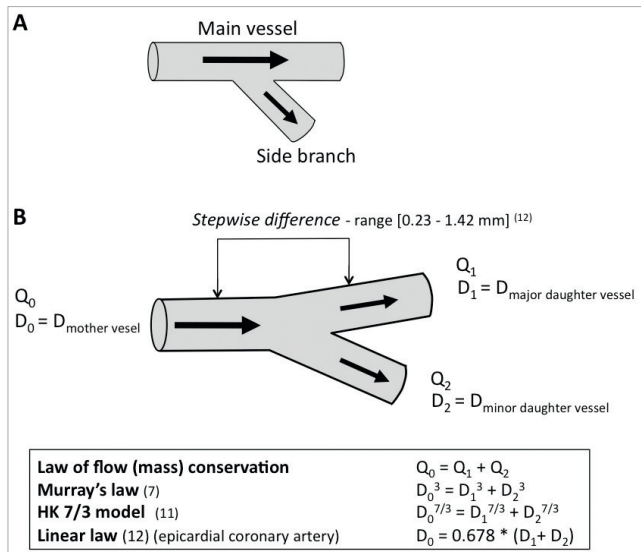


Figure 2. Evolution of arterial bifurcation schema. A) A conventional schema, in which the "main vessel" diameter is conserved before and after the origin of "side branch", which is false. B) True representation of a bifurcation, with a mother vessel dividing into two daughter vessels. Strict relations are obtained between the flow rates and diameters of the three vessels, in agreement with the law of conservation of mass (or flow). The diameter of the mother vessel is systematically greater than that of the larger daughter vessel. A fundamental fact follows from this: the greater the difference in diameter between the two daughter vessels, the greater the systematic stepwise difference between the diameters of the mother and major daughter vessels.

Bifurcation geometry/function relation for simple fractal

According to the law of conservation of mass, the sum of flow rates in two daughter vessels equals the flow rate in mother vessel as:

$$Q_m = Q_{d1} + Q_{d2} \quad [1]$$

where m , $d1$ and $d2$ correspond to the mother vessel and two daughter vessels. From the flow-diameter scaling relation in Ref. 11 (i.e., 7/3 law), we obtain:

$$Q_m = K \cdot D_m^{2\frac{1}{3}}, Q_{d1} = K \cdot D_{d1}^{2\frac{1}{3}}, Q_{d2} = K \cdot D_{d2}^{2\frac{1}{3}} \quad [2]$$

The combination of Eqs. [1] and [2] leads to:

$$D_m^{2\frac{1}{3}} = D_{d1}^{2\frac{1}{3}} + D_{d2}^{2\frac{1}{3}} \quad [3]$$

If $D_{d1} = D_{d2} = D_d$, then Eq. [3] can be written as:

$$R = \frac{D_m}{2 \cdot D_d} = 2^{-\frac{4}{7}} = 0.673 \quad [4]$$

Equation [4] is very similar to the experimentally measured $R=0.678$ in coronary epicardial bifurcations¹².

As demonstrated by this simple example, the bifurcation geometry is closely related to flow distribution as dictated by the law of mass conservation and the minimum energy hypothesis and it reflects a fractal geometry of the coronary branching.

Coronary bifurcations ensure the haemodynamic function

The branching pattern is asymmetric in the coronary arterial tree which results in heterogeneous distribution of flow at bifurcations^{13,14}

and in the myocardium¹⁵. The asymmetry is predictable and quantifiable, however, and lends the flow to scale with blood volume, myocardial mass, sum of arterial lengths and vessel diameter. The latter scales generally as a power-law exponent (7/3) and simplifies to $D_m = 0.678 * (D_{d1} + D_{d2})$ in the case of Y-bifurcations as shown above.

Bifurcations divide the blood flow and change the velocity profile

A bifurcation causes incoming blood flow to deviate from its initial streamline in the mother vessel. This leads to a force of inertia, which creates a centrifugal force. The centrifugal force, in turn, induces a new velocity gradient. The higher speeds occurs on the internal parts of the daughter vessels in continuity with the carina and a significant reduction in speed occurs on the external part of the arterial wall of the daughter vessels facing the carina. The carina thus acts as a flow divider. On the arterial walls facing the carina, there is thus low wall shear stress with areas of recirculation. Similar haemodynamic disturbances are also found in curved vascular segments where the interior part of the bend experiences low shear stress. The same phenomenon is found in aerial observation of a meandering river, with silting occurring exactly in the interior of each bend (Figure 3a, b). The distribution of circulating flow velocities in an artery is not homogeneous, but rather has a parabolic pattern (Hagen-Poiseuille flow) with maximal along the geometric axis of the vessel, and diminishing towards the arterial wall (Figure 3c). The velocity (or shear-stress) gradient is the difference between two contiguous velocities. Thus, the shear-stress profile within an artery is relatively

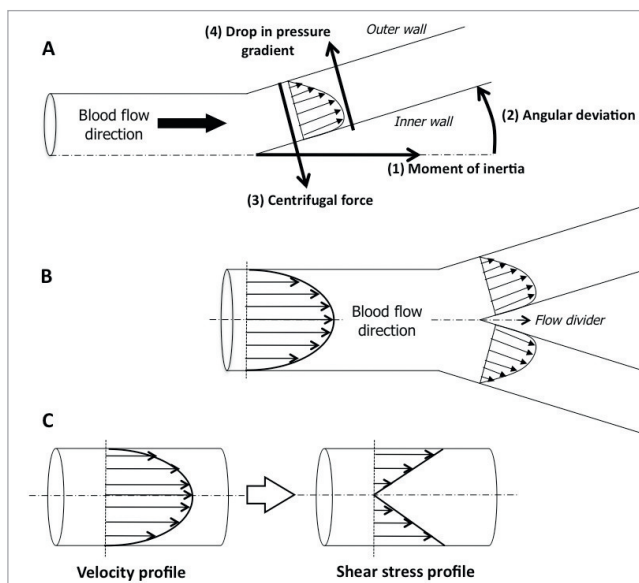


Figure 3. Schematic analysis of bifurcation impact on fluid dynamics. A) Laminar flow in an artery induces a force of inertia (1) in the direction of flow; a sudden change in direction characterised by an angular deviation (2) induces a centrifugal force (3) which creates a pressure gradient at the exit from the change in direction. B) Description of fluid dynamics changes from symmetric laminar flow before the bifurcation to asymmetric flow gradients after division of the flow. C) The flow velocity profile is associated with a shear stress profile, corresponding to the derivative of the velocities from their radial position.

characteristic; i.e., zero along the geometric axis of the artery and maximal in contact with the arterial wall. The velocity gradient in contact with the wall is called wall shear stress (Figure 3c) where the steeper the gradient, the greater the differential velocity¹⁶. Endothelial cells are sensitive to shear stress via their cytoskeletal mechano-receptors¹⁷.

Bifurcations induce local flow disturbance

Figure 4 clearly shows that the flow divider (i.e., carina) of a bifurcation is the region of elevated wall shear stress and has a high spatial gradient of wall shear stress. In contrast, the arterial walls facing the carina (particularly if curved) experience low or oscillatory wall shear stress¹⁸⁻²⁰. Areas of low wall shear stress are located at the entry to the bifurcation in the mother vessel, and on the two sides of daughter vessels facing the carina. In a curved arterial segment, regions of low wall shear stress exist in the internal part of the curvature^{16,19-21}. The sinuous nature of coronary arteries thus entails areas of low shear stress.

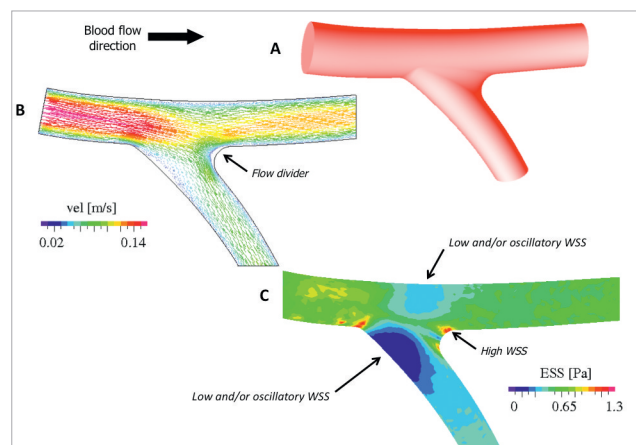


Figure 4. Numeric simulation in coronary bifurcations. A) The coronary bifurcation model respects a fractal geometry. B) Map of velocity profile, showing the preferential route towards the flow divider induced by the force of inertia. C) Map of wall shear stress (WSS) showing two contrasting regions at the flow divider where WSS is low, regions where flow is very slow and/or oscillatory.

Bifurcations are the focus of mechano-cellular and biological effects. In regions of recirculation and/or low shear stress there is increased predilection to atherogenesis. Endothelial cells have mechano-receptors which render them sensitive to wall shear stress. A drop in wall shear stress induces specific responses including prothrombotic, pro-migration, pro-apoptotic action that promote cell growth (angiotensin 2, TDGF, endothelin-1). Moreover, low shear-stress regions alter the geometry of endothelial cells, making their elongated pavement heterogeneous and polygonal which result in uncovered areas that become the focus of cell migration and platelet adhesion¹⁷.

Bifurcations act as atherogenesis sites

Several groups have demonstrated the relation between the initial stages of atherogenesis and low shear stress regions as the preferential sites of cellular adhesion protein (VCAM-1) expression²².

Cheng et al²³ experimentally demonstrated that atherosclerotic lesion size and vulnerability are determined by the patterns of fluid shear stress. Consequently, bifurcations show specific atherosclerotic regions according to wall shear stress distribution. The flow disturbances at a bifurcation initiate the development of atherosclerosis, which in turn induce additional region of low shear stress downstream of the plaque²⁴. Subsequent plaque growth results in endoluminal obstruction which increases flow velocity and normalises wall shear stress in the proximal part of the plaque and in the obstruction itself. This, however, creates a further downstream region of low or oscillatory wall shear stress. Initial radial plaque growth thus progressively induces downstream longitudinal growth.

The type of wall shear stress (low or oscillatory) can also affect rupture vulnerability in plaque evolution, as shown by Cheng²³. Regions of low, rather than oscillatory, shear stress promote vulnerability by significantly increasing the levels of macrophages, lipid inclusions and MMP activity and thereby reducing collagen content. Once a plaque is well developed in a bifurcation, its obstructive effect locally elevates upstream wall shear stress, inducing plaque rupture due to the increased parietal stress²⁵.

Since bifurcations occur throughout the epicardial coronary tree accompanied by distribution of wall shear stress patterns, they have specific lesion vulnerability. Cheruvu et al²⁶ mapped the spatial distribution of complex ostial coronary lesions distal to the LAD, LCX and RCA arteries. Most fibro-atheromatous lesions lie in the first 4 cm of the LAD and the first 4.5 cm of the LCX, but are distributed over more than 10 cm in the right coronary (which has large proximal and distal bends). Thin-cap and ruptured plaques also cluster in regions of bifurcation (proximal LAD) or in regions of significant curvature (proximal segment of the LCX and the two bends of the RCA).

Bifurcation stenting should respect geometric rules

Interventional cardiologists can make practical use of the principles underlying bifurcation geometry in normal vessels.

- 1) Angiographic underestimation of left main coronary artery (LMCA) stenosis can be corrected by applying the geometric rule to obtain a theoretic LMCA diameter, thereby unmasking any diffuse atherosclerotic LMCA disease, or to quantify focal stenosis more precisely where adjacent segments are also pathological²⁷.
- 2) The outflow to inflow ratio is also linked to the respective diameters by HK 7/3 power law, showing the functional relevance of certain side-branches that are often dismissed as functionally secondary (Figure 5).
- 3) The systematic difference between major daughter vessel and mother vessel diameter (the greater the difference, the closer the two daughter-vessel diameters) leads to acute proximal stent malapposition that should be taken into account in interventional management of bifurcations¹². A coronary bifurcation bench test consistent with fractal rule (for example) provides a view of proximal stent malapposition analysed on microfocus X-ray tomography²⁸. A stent which has the diameter of the major

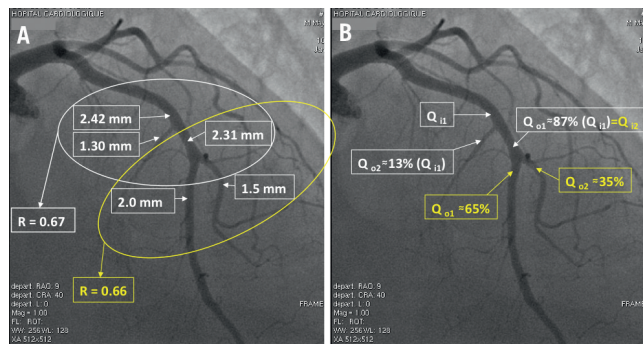


Figure 5. Demonstration of variations in LAD artery geometry and flow after departure of a first septal artery and a diagonal artery. A) The variations in diameter agree with the linear law ($D_{\text{mother vessel}} = 0.678 * (D_{\text{daughter vessel}1} + D_{\text{daughter vessel}2})$), to within the intrinsic variations in quantitative angiographic measurement. B) The outflow-to-inflow ratio is also related to the respective diameters by Murray's cube law, showing the functional relevance of certain side branches often dismissed as of secondary importance.

daughter-vessel will systematically show proximal malapposition in the mother vessel (Figure 6). The degree of this malapposition (ΔD) can easily be calculated in advance of implantation:

$$\Delta D = D_{\text{mother vessel}} - D_{\text{major daughter vessel}}$$

An additional inflation of the proximal segment by a balloon having the diameter of the mother vessel is a well-adapted practice. A final kissing balloon inflation can also mechanically correct the malapposition at the cost of asymmetric deformation of the mother vessel induced by the proximal juxtaposition of the two balloons (Figure 7).

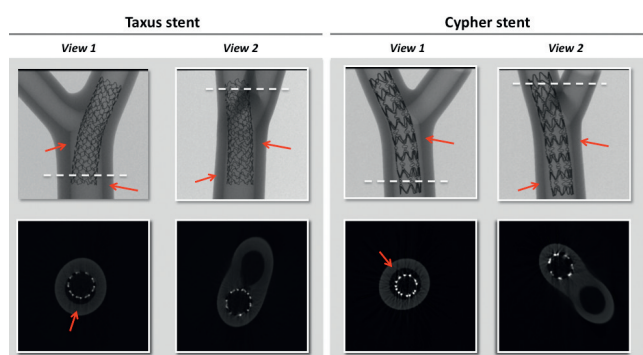


Figure 6. Stent implantation in left main bifurcation fractal bench test. We performed a left main bifurcation bench test respecting fractal geometry, in 55 shA crystal PVC with the rheology of a 1-mm thick coronary artery (Young's modulus: 500 kPa). Mother-vessel diameter: 4.1 mm; daughter-vessel diameters: 3.0 mm; bifurcation angle: 67°. Two TAXUS Liberty® (Boston Scientific, Natick, MA, USA) and Cypher Select® (Cordis Corporation, Warren, NJ, USA) stents having the daughter-vessel diameter (3.0 mm) were implanted at 16 bars. The correct strategy is to use a stent with a diameter adapted to the D of the main daughter vessel to avoid possible coronary dissection. Acute proximal stent malapposition was systematically seen on microfocus X-ray tomography. The expected stepwise difference of 1.1 mm was found between the mother- and daughter-vessel diameters.

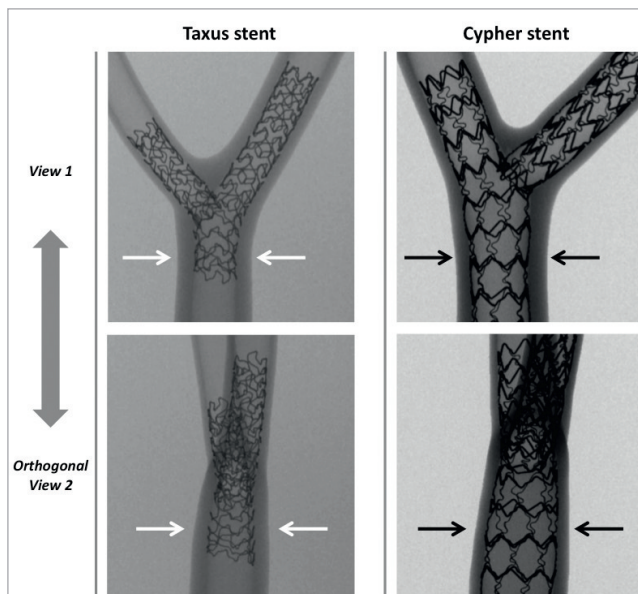


Figure 7. Final kissing balloon inflation after stent implantation in left main bifurcation fractal bench test. Correction of the systematic acute proximal stent malapposition induced by the expected difference in mother- and major daughter-vessel diameters (main axis) by final kissing balloon inflation. The final kissing balloon correct the ostium of the side branch and oversize the stent in the mother vessel. This strategy is largely accepted by the interventional cardiology community.

Summary

Coronary bifurcations are transitional junctions that allow the divergence of the system to nourish the myocardium. The apparent complexity of the tree consists of a self-similar pattern of branching (i.e., a fractal geometry), based on energetic efficiency (principle of minimum work for blood transport). The bifurcation is a strategic nexus of geometry, fluid dynamics and rheology. Atherogenesis, atherosclerosis, plaque vulnerability and thrombosis are closely associated with the geometric and fluid dynamics factors at the bifurcation. Moreover, stenting of bifurcations also may contribute to additional haemodynamic disturbances. Interventional management of bifurcations should therefore restore optimal flow and minimise further haemodynamic disturbances by obeying the rules of geometry and hence function.

"In anything at all, perfection is finally attained not when there is no longer anything to add, but when there is no longer anything to take away"

Antoine de Saint-Exupéry

References

1. Kassab GS. Functional hierarchy of coronary circulation: direct evidence of a structure-function relation. *Am J Physiol Heart Circ Physiol* 2005;289:H2559-2565.
2. Mandelbrot B. *Fractals: form, chance, and dimensions*. San Francisco: Freeman; 1977.
3. Bassingthwaite JB, Liebovitch LS, West BJ. *Fractal physiology*. 1994; New-York:Oxford University Press.

4. Kassab GS, Rider CA, Tang NJ, Fung YC, Bloor CM. Morphometry of pig coronary arterial trees. *Am J Physiol* 1993;265:H350-H365.
5. Zamir M. Fractal dimensions and multifractality in vascular branching. *J theor Biol* 2001;212:183-190.
6. Ito K, Shinozaki Y, Hyodo K, Ando M, Umetani K, Tanioka K, Kubota M, Abe S, Handa S, Nakazawa H. Branching patterns of intramural coronary vessels determined by microangiography using synchrotron radiation. *Am J Physiol*. 1999;276:2262-2267.
7. Murray CD. The physiological principle of minimum work. The vascular system and the cost of blood volume. 1926; *Proc Natl Acad Sci USA*; 12:207-214.
8. Zhou Y, Kassab GS, Molloy S. On the design of the coronary arterial tree: a generalization of Murray's law. *Phys Med Biol* 1999;44:2929-2945.
9. Zhou Y, Kassab GS, Molloy S. In vivo validation of the design rules of the coronary arteries and their application in the assessment of diffuse disease. *Physics in Med and Bio* 2002;47: 977-993.
10. Kassab GS. Design of Coronary Circulation: The Minimum Energy Hypothesis. *Comput Methods Appl Mech Eng* 2007;196:3033-3042.
11. Huo Y, Kassab GS. A scaling law of vascular volume. *Biophys J* 2009;96:347-353.
12. Finet G, Gilard M, Perrenot B, Rioufol G, Motreff P, Gavitt L, Prost R. Fractal geometry of arterial coronary bifurcations: a quantitative coronary angiography and intravascular ultrasound analysis. *EuroIntervention* 2007;3:10-17.
13. Kalsho G, Kassab GS. Bifurcation asymmetry of the porcine coronary vasculature and its implications on coronary flow heterogeneity. *Am J Physiol Heart Circ Physiol* 2004;287:H2493-H2500.
14. Kaimovitz B, Huo Y, Lanir Y, Kassab GS. Diameter asymmetry of porcine coronary arterial trees: structural and functional implications. *Am J Physiol Heart Circ Physiol* 2008;294, H714-723.
15. Huo Y, Kaimovitz B, Lanir Y, Hoffman JIE, Kassab GS. Biophysical Model of Spatial Heterogeneity of Myocardial Flow. *Biophys J*. 2009;96:4035-43.
16. Soulis JV, Farmakis TM, Giannoglou GD, Louridas GE. Wall shear stress in normal left coronary artery tree. *J Biomech*. 2006;39:742-749.
17. Traub O, Berk BC. Laminar shear stress: mechanisms by which endothelial cells transduce an atheroprotective force. *Arterioscler Thromb Vasc Biol*. 1998;18:677- 685.
18. Giannoglou GD, Soulis JV, Farmakis TM, Giannakoulas GA, Parcharidis GE, Louridas GE. Wall pressure gradient in normal left coronary artery tree. *Med Eng Phys*. 2005;27:455-464
19. Huo Y, Wischgoll T, Kassab GS. Flow patterns in three-dimensional porcine epicardial coronary arterial tree. *Am J Physiol Heart Circ Physiol* 2007;293:H2959-H2970.
20. Huo Y, Choy JS, Svendsen, M, Sinha AK, Kassab GS. Effects of vessel compliance on flow pattern in porcine epicardial right coronary arterial tree. *J Biomech* 2009;42:594-602.
21. Huo Y, Guo X, Kassab GS. The flow field along the entire length of mouse aorta and primary branches. *Ann Biomed Eng* 2008;36:685-699.
22. Suo J, Ferrara DE, Sorescu D, Guldberg RE, Taylor WR, Giddens DP. Hemodynamic Shear Stresses in Mouse Aortas: Implications for Atherogenesis. *Arterioscler. Thromb. Vasc. Biol*. 2007;27:346-351.
23. Cheng C, Tempel D, Van Haperen R, Van Der Baan A, Grosveld F, Daemen MJAP, Krams R, De Crom R. Atherosclerotic lesion size and vulnerability are determined by patterns of fluid shear stress. *Circulation* 2006;113:2744-2753.

24. Gijsen FJH, Wentzel JJ, Thury A, Mastik F, Schaar JA, Schuurbiers JCH, Slager CJ, Van Der Giessen WJ, De Feyter P, Van Der Steen AFW, Serruys PW. Strain distribution over plaques in human coronary arteries relates. *Am J Physiol Heart Circ Physiol* 2008;295:H1608-H1614.
25. Fukumoto Y, Hiro T, Fujii T, Hashimoto G, Fujimura T, Yamada J, Okamura T, Matsuzaki M. Localized elevation of shear stress is related to coronary plaque rupture: a 3-dimensional intravascular ultrasound study with in vivo color mapping of shear stress distribution. *J Am Coll Cardiol* 2008;51:645-50.
26. Cheruvu PK, Finn AV, Gardner C, Caplan J, Goldstein J, Stone GW, Virmani E, Muller JA. Frequency and distribution of thin-cap fibroatheroma and ruptured plaques in human coronary arteries. *JACC* 2007;50:940-949.
27. Motreff P, Gilard M, Caussin C, Ouchtane L, Souteyrand G, Finet G. Diffuse atherosclerotic left main coronary artery disease unmasked by fractal geometric law applied to quantitative coronary angiography: angiographic and intravascular ultrasound study. *EuroIntervention* 2010;5:1-7.
28. Guérin P, Pilet P, Finet G, Gouëffic Y, N'Guyen JM, Crochet D, Tijou I, Pacaud P, Loirand G. Drug-eluting stents in bifurcations: bench study of strut deformation and coating lesions. *Circ Cardiovasc Interv* 2010; 3:120-6.